



1     **Investigation of An Extreme Rainfall Event during 8-12 December 2018 over**  
2             **Central Vietnam. Part I: Analysis and Cloud-Resolving Simulation**

3

4                             Chung-Chieh Wang and Duc Van Nguyen\*

5

6     Department of Earth Sciences, National Taiwan Normal University, Taipei, Taiwan

7

8     Corresponding author address: Duc Van Nguyen ([nguyenvanduc\\_t57@hus.edu.vn](mailto:nguyenvanduc_t57@hus.edu.vn)),

9     Department of Earth Sciences, National Taiwan Normal University, No. 88, Sec. 4, Ting-  
10     Chou Rd., Taipei 11677, Taiwan

11     **Highlights:**

- 12         • A record-breaking rainfall event over central Vietnam is investigated and its  
13             simulation result using a cloud-resolving model is evaluated
- 14         • Key factors in this event include the combined effect of northeasterly wind that  
15             originated from northern China, easterly wind, local topography, and high sea surface  
16             temperature
- 17         • A cloud-resolving model is applied to study an extreme rainfall event in central  
18             Vietnam, and the results are very impressive



19

## Abstract

20 An extreme rainfall event occurred from 8 to 12 December 2018 along the coast of central  
21 Vietnam. The observed maximum rainfall amount in 72 h was over 900 mm and set a new record,  
22 and the associated heavy losses were also significant. The analysis of this event shows some key  
23 factors for its occurrence: (1) The interaction between the strong northeasterly winds, blowing from  
24 the Yellow Sea into the northern South China Sea (SCS), and easterly winds over the SCS in the  
25 lower troposphere (below 700 hPa). This interaction created strong low-level convergence, as the  
26 winds continued to blow into central Vietnam against the Truong Son Range, resulting in forced  
27 uplift over the coastal plains due to the terrain's barrier effect. As a consequence, heavy rainfall  
28 occurred along the coast. (2) The strong easterly wind played an important role in transporting  
29 moisture from the western North Pacific across the Philippines and the SCS into central Vietnam.  
30 (3) The Truong Son Range also contributed to this event due to its barrier effect. (4) In addition to  
31 cumulonimbus, the low-level precipitating clouds such as nimbostratus clouds were also major  
32 contributors to rainfall accumulation for the whole event.

33 The Cloud-Resolving Storm Simulator (CReSS) was employed to simulate this record-  
34 breaking event at high resolution, and the overall rainfall can be captured quite well not only in  
35 quantity but also in its spatial distribution (with a Fractions Skill Score  $\approx 0.7$  and Threat Score  $> 0$   
36 at 700 mm for 72 h rainfall). Thus, the CReSS model is shown to be a useful tool for both research  
37 and forecasts of heavy rainfall in Vietnam. The model performed better for the rainfall during 9-10  
38 but not as good on 11 December. In the sensitivity test without the terrain, the model did not  
39 generate nearly as much rainfall for this event. Thus, the test confirms the important role played by  
40 the local topography for the occurrence of this event.

41 Keywords: Extreme rainfall, central Vietnam, cloud-resolving model.

42



## 43 **1 Introduction**

44 Heavy to extreme rainfalls are natural disasters that often cause deaths, flooding, landslides,  
45 and erosion. Vietnam is one of the most disaster-prone countries in the world with many different  
46 types of natural hazards. In the country, central Vietnam is most affected by natural disasters and  
47 climate change, with frequent occurrences of rainstorms and extreme rainfalls. For example, during  
48 8-12 December 2018, an extreme rainfall event (hereafter abbreviated as the D18 event) occurred  
49 along the coast of central Vietnam. The peak 72-h accumulated rainfall (from 1200 UTC 8 to 1200  
50 UTC 11 Dec) at some stations exceeds 800 mm (Fig. 1d). Among the stations, Da Nang (16.0° N,  
51 108.2° E, cf. Figs. 1a,b) recorded 24-h rainfall amounts greater than 600 mm on 9 December and  
52 over 300 mm the next day. This extreme event resulted in 13 deaths, an estimated 1200 houses  
53 inundated, around 12,000 hectares of crops destroyed, some 160,000 livestock killed and many  
54 other economic losses (Tuoi Tre news, 2018). Furthermore, according to climate change and sea-  
55 level rise scenarios for Vietnam, extreme precipitation events will increase in both their frequency  
56 and intensity in the future (Tran *et al.*, 2016). Hence, how to improve the ability in the quantitative  
57 precipitation forecast (QPF) of heavy-rainfall events over central Vietnam is very important.

58 In this study, central Vietnam is referred to as the area between 14.7° N and 18° N (Fig. 2a). Its  
59 eastern boundary is the South China Sea (SCS), and the western boundary is the border to Laos,  
60 where the Truong Son Range (also known as the Annamite Range) runs parallel to the coast. The  
61 central Vietnam includes Quang Binh, Quang Tri, Thua Thien Hue, Da Nang city, Quang Nam, and  
62 a part of Quang Ngai province. The topography is characterized by high mountains (< 3000 m),  
63 highlands, narrow coastal plain with the narrowest place less than 100 km in width (east-west), and  
64 gradually lowers from the west to the east (Fig. 2b). Most of the population and cities are  
65 concentrated along the coastal plain. By these characteristics of steep topography, when heavy rain  
66 occurs, it often leads to flooding and causes great damages to people and the environment.

67

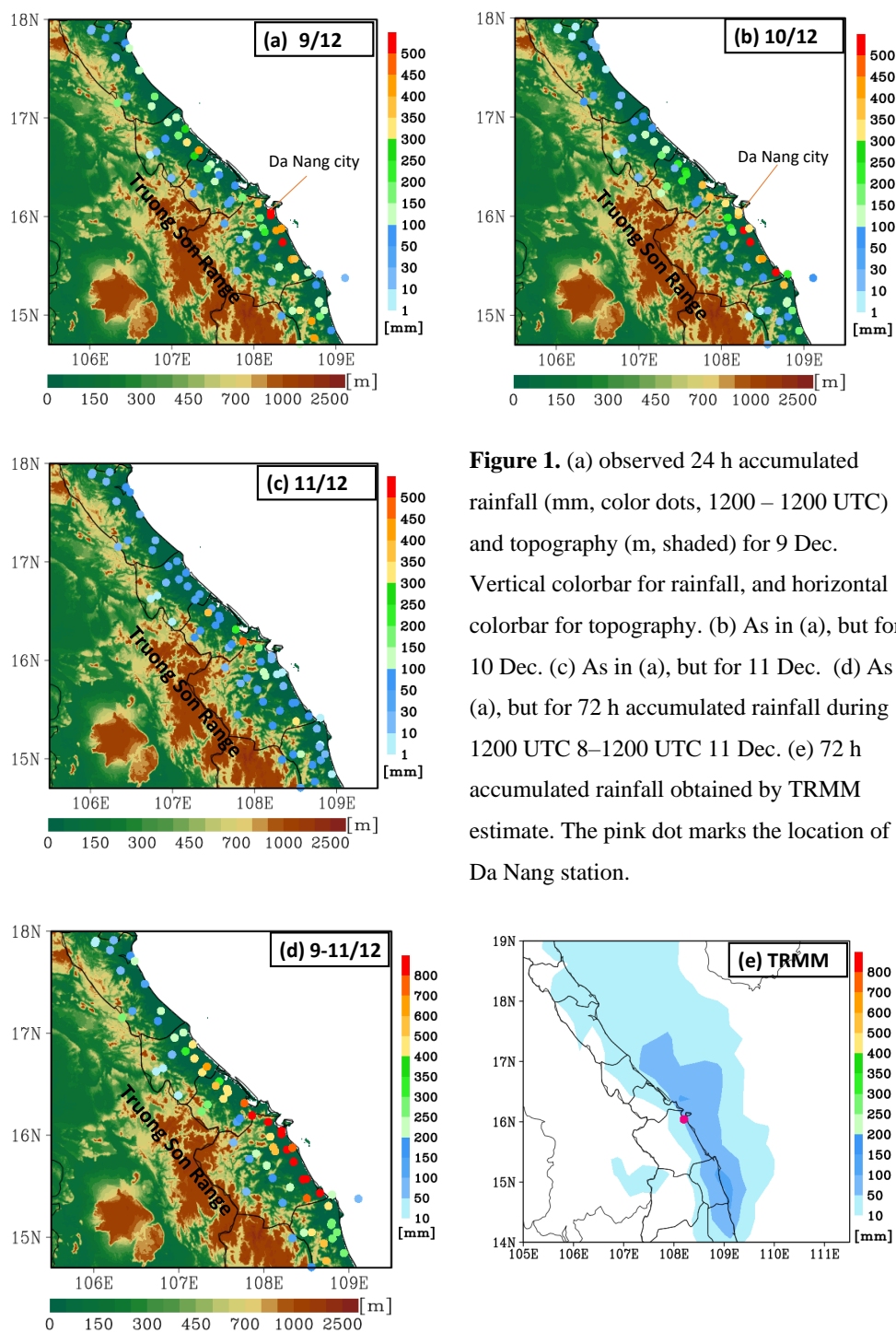
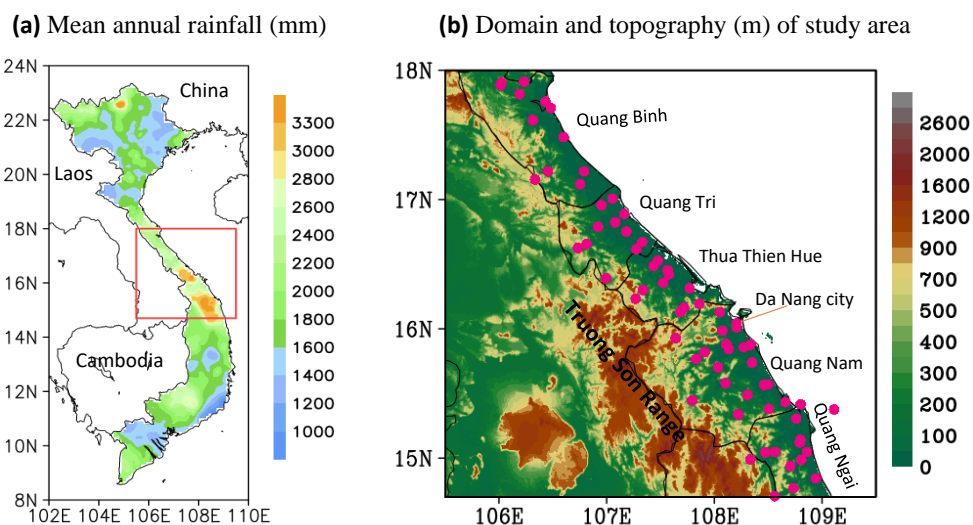


**Figure 1.** (a) observed 24 h accumulated rainfall (mm, color dots, 1200 – 1200 UTC) and topography (m, shaded) for 9 Dec. Vertical colorbar for rainfall, and horizontal colorbar for topography. (b) As in (a), but for 10 Dec. (c) As in (a), but for 11 Dec. (d) As in (a), but for 72 h accumulated rainfall during 1200 UTC 8–1200 UTC 11 Dec. (e) 72 h accumulated rainfall obtained by TRMM estimate. The pink dot marks the location of Da Nang station.



68 **Figure 2.** (a) Mean annual rainfall distribution (mm) in Vietnam from 1980 to 2010, obtained from  
69 the Vietnam Gridded Precipitation (VnGP) data, and the study area of central Vietnam (red box).  
70 (b) The domain and topography (m) of central Vietnam. Pink dots mark the locations of rain-gauge  
71 stations.

72 Climatologically, the central part of Vietnam is the country's rainiest region and is strongly  
73 affected by heavy to extreme rainfall, with average annual precipitation ranging from 2400 to over  
74 3300 mm (1980–2010, Fig. 2a). The main rainy season in this region is from late fall to early winter  
75 (Yokoi and Matsumoto, 2008; Chen *et al.*, 2012).

76 Past studies have shown some main factors that can lead to heavy rainfall in central Vietnam,  
77 such as (1) the combined effect of cold surges that originate from northern China, (2) tropical  
78 depressions, and (3) local topography (Bui, 2019; Yokoi and Matsumoto, 2008; Chen *et al.*, 2012;  
79 Nguyen-Le and Matsumoto, 2016; van der Linden *et al.*, 2016). According to these studies, a cool,  
80 dry continental surface high pressure system (known as the Siberian high-pressure system)  
81 gradually establishes over the continental East Asia after boreal summer in October–November.  
82 This high-pressure system's intensification and southeastward amplification lead to an episodic



83 southward progression of cold surge into the tropics. The interaction of this cold surge and  
84 preexisting tropical disturbance over the SCS and the topography in central Vietnam can bring large  
85 amounts of rainfall along the east-central coast through orographic rainfall processes.

86 According to [Wang et al. \(2017\)](#), Vietnam is impacted by about 4-6 typhoons per year.  
87 [Nguyen-Thi et al. \(2012\)](#) investigated the characteristic of tropical cyclone rainfall over Vietnam in  
88 the climatology. Their results show that the tropical cyclone rainfall amount is concentrated in  
89 central Vietnam, peaking between October and November. [Takahashi et al. \(2009\)](#) performed a  
90 long-term simulation for September (from 1966 to 1995) using a high-resolution model. They found  
91 that the observed long-term decrease in September rainfall is due to the weakening of tropical  
92 cyclone activity over the Indochina Peninsula. As for the impacts of El Niño-Southern Oscillation  
93 (ENSO), some studies have examined the linkages between rainfall in Vietnam and ENSO, and  
94 suggested more (less) rainfall during La Niña (El Niño) years. For example, [Yen et al. \(2010\)](#)  
95 analyzed the interannual variation of the rainfall in fall over central Vietnam, and their results  
96 indicated a negatively correlated relationship between rainfall in central Vietnam and the sea  
97 surface temperature over the NINO3.4 region. Besides, [Vu et al. \(2015\)](#) investigated the effects of  
98 ENSO on fall rainfall in central Vietnam and concluded that central Vietnam has more (less)  
99 rainfall in La Niña (El Niño) years. Finally, [Wu et al. \(2012\)](#) analyzed the Madden-Julian  
100 Oscillation (MJO) activity from September to November for 30 years (1981-2010) over Vietnam  
101 and showed that the MJO is also an important factor in the formation of extreme precipitation  
102 events in central Vietnam.

103 From the review above, the important mechanisms for the heavy rainfall in some previous  
104 events over central Vietnam are revealed. However, the D18 event set a new historical rainfall  
105 record and left with heavy losses in central Vietnam. As the magnitude of the D18 event surpassed  
106 all past events, several questions are therefore raised: What mechanisms caused this record-  
107 breaking event at such a magnitude? Was its mechanism similar to those in previous events? Or, it



108 was a different one. How important was the role played by local terrain in this event? From a  
109 forecast perspective, one related question would be whether a cloud-resolving or high-resolution  
110 model is capable of reproducing the D18 event? The answers to these questions will help improve  
111 our understanding on the mechanisms that cause heavy rainfall in central Vietnam, as well as on the  
112 predictability of such events in the future. Hence, the present study was carried out with an aim to  
113 answer the above questions. The remainder of this paper is organized as follows: Section 2  
114 describes the datasets and methodology used in the study. The analysis and modeling results are  
115 presented in Section 3 and 4, respectively. Finally, the conclusions are given in Section 5.

## 116 **2 Data and Methodology**

### 117 **2.1 Data**

#### 118 *2.1.1 NCEP GDAS/FNL Global Gridded Analyses and Forecasts*

119 This dataset is provided freely by the National Centers for Environmental Prediction (NCEP).  
120 In this study, this dataset is used as the initial and boundary conditions (IC/BCs) for the cloud-  
121 resolving model (CRM) simulation. The data are on a  $0.25^\circ \times 0.25^\circ$  latitude-longitude grid with 26  
122 levels extending from the surface to 20 hPa. The data period is from 0600 UTC 8 December to 0000  
123 UTC 13 December 2018, at 6-h intervals. Parameters include geopotential height, zonal and  
124 meridional wind components, pressure, temperature, and relative humidity. The dataset and its  
125 detailed information are available at <https://rda.ucar.edu/datasets/ds083.3>.

#### 126 *2.1.2 The fifth generation ECMWF reanalysis data (ERA5)*

127 The ERA5 is the fifth-generation reanalysis dataset, developed by the European Centre for  
128 Medium-range Weather Forecasts (ECMWF) to replace the ERA-Interim reanalysis. We have used  
129 these data to delineate the synoptic weather patterns during the D18 event. The horizontal resolution  
130 of this dataset is  $0.25^\circ \times 0.25^\circ$  latitude-longitude at 22 selected levels from 1000 to 100 hPa and  
131 including the surface. Parameters include zonal and meridional wind components, geopotential



132 height, specific humidity, relative humidity, temperature, vertical velocity, mean sea level pressure,  
133 and sea surface temperature. The dataset was downloaded from 0000 UTC 8 to 1800 UTC 11  
134 December 2018 at 6-h intervals ([Hersbach et al., 2018a,b](#)).

### 135 *2.1.3 Observation data*

136 The daily observed rainfall data (1200–1200 UTC, i.e., 1900–1900 LST) from 8 to 12  
137 December 2018 at 69 automated gauge stations across central Vietnam are used for case overview  
138 and verification of model results. This dataset is provided by the Mid-central Regional Hydro-  
139 Meteorological Centre, Vietnam.

### 140 *2.1.4 Satellite data*

#### 141 (a) TRMM (TMPA) rainfall estimates

142 The TRMM multi-satellite precipitation estimates (3B42, version 7, [Huffman et al., 2016](#)) are  
143 freely provided by the NASA Goddard Earth Sciences (GES) Data and Information Services Center  
144 (DISC). The horizontal resolution of this dataset (level 3) is  $0.25^\circ \times 0.25^\circ$  latitude-longitude and the  
145 time resolution is every 3 h. In this study, this dataset was downloaded from 1200 UTC 8 to 1200  
146 UTC 11 December 2018 to analyze the D18 event.

#### 147 (b) The Himawari satellite images

148 The color-enhanced infrared imageries are designed mainly for the detection of convective  
149 clouds, including those from the Himawari-8 satellite. The different colours represent different  
150 cloud-top heights. Therefore, we have used these images to discern deep convection in convective  
151 clouds and precipitating clouds based on their characteristics. In this study, the dataset was  
152 downloaded from the Central Weather Bureau website, Taiwan, with a time resolution of 1 h.

### 153 *2.1.5 Radar data*





154 The column-maximum radar reflectivity data are one indispensable data source to identify  
155 precipitation and verify model results. The reflectivity data (in dBZ) cover a wide range and the  
156 values indicate rainfall intensity (the higher the dBZ, the stronger the intensity of precipitation).  
157 Therefore, we used the column-maximum radar reflectivity data over central Vietnam at 1-h  
158 intervals over 8-11 December 2018 to estimate the rainfall intensity during the D18 event. This  
159 dataset is provided by the Mid-central Regional Hydro-Meteorological Centre of Vietnam.

#### 160 *2.1.6 The Vietnam Gridded Precipitation (VnGP) Dataset.*

161 The VnGP data are derived base on the daily observed data from 481 rain gauges cross  
162 Vietnam. This dataset has a resolution of  $0.1^\circ$  and covers the period of 1980-2010 (Nguyen-Xuan et  
163 al., 2016). In this study, this dataset is used to depict the rainfall climatology in Vietnam.

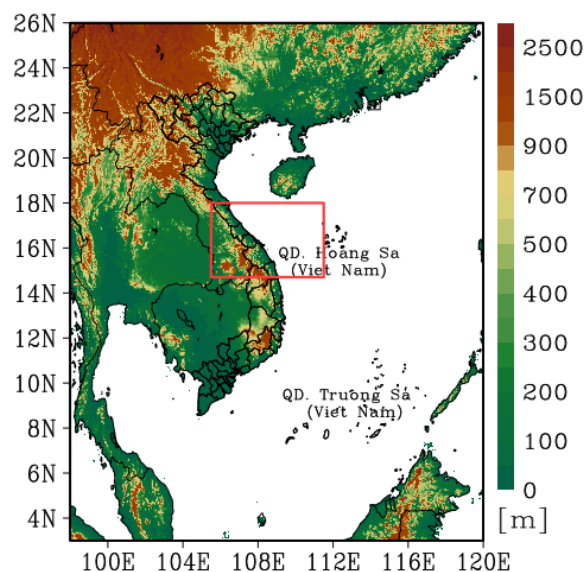
## 164 **2.2 Model description and experiment setup**

165 The Cloud Resolving Storm Simulator (CReSS, version 3.4.2), developed by Nagoya  
166 University, Japan (Tsuboki and Sakakibara, 2002, 2007) is used for numerical simulation of the  
167 D18 event. This model is a non-hydrostatic and compressible cloud model, designed for simulation  
168 of weather events at high (cloud-resolving) resolution. In the model, the cloud microphysics is  
169 treated explicitly at the user-selected degree of complexity, such as the bulk cold-rain scheme with  
170 six species: vapor, cloud water, cloud ice, rain, snow, and graupel (Lin et al., 1983; Cotton et al.,  
171 1986; Murakami, 1990, 1994; Ikawa and Saito, 1991). The CReSS model is also designed to be run  
172 on large computers at high efficiency. Heretofore, this model has been applied to study tropical  
173 cyclones, heavy rainfall events, and many other convective systems (e.g., Ohigashi and Tsuboki,  
174 2007; Yamada et al., 2007; Akter and Tsuboki, 2010, 2012; Wang et al., 2015).

175 To study the D18 event and investigate the role played by the local terrain in this event using  
176 the CReSS model, two experiments were performed starting from the same initial time of 0600  
177 UTC 8 December 2018. One is the control simulation (CTRL) with full terrain and the other is the



178 sensitivity test without the terrain (NTRN). The simulation domain is depicted in Fig. 3. The basic  
 179 information of these two experiments, including the domain setup and model configuration, is listed  
 180 in Table 1.



181  
 182 **Figure 3:** The simulation domain of the CReSS model and topography (m) used in this study. The  
 183 red box marks the study area.

184 **Table 1.** The basic information of experiments.

Model domain	3°–26°N; 98°–120°E
Grid dimension ( $x, y, z$ )	912 × 900 × 60
Grid spacing ( $x, y, z$ )	2.5 km × 2.5 km × 0.5 km*
Projection	Mercator
Simulation length	114 h
Topography (for CTRL) and sea surface temperature (SST)	Real at (1/120)° and NCEP analyses (0.25° × 0.25°)
Cloud microphysics	Bulk cold-rain scheme (six species)

185



186 **2.3 Verification of model rainfall**

187 In order to verify the model-simulated rainfall, some verification methods are used, including  
 188 (1) visual comparison between the model and the observation (from the 69 automated gauges over  
 189 the study area), and (2) the objective verification using categorical skill scores at various rainfall  
 190 thresholds from the lowest at 0.05 mm up to 900 mm for three-day total. These scores are listed in  
 191 Table 2 along with their formulas, perfect value, and worst value, respectively. To apply these  
 192 scores at a given threshold, the model and observed value pairs at all verification points (gauge sites  
 193 here, = N) are first compared and classified to construct a 2 × 2 contingency table (Wilks, 2006). At  
 194 any given site, if the event takes place (reaching the threshold) in both model and observation, the  
 195 prediction is considered a hit (H). If the event occurs only in observation but not the model, it is a  
 196 miss (M). If the event is predicted in the model but not observed, it is a false alarm (FA). Finally, if  
 197 both model and observation show no event, the outcome is correct negative (CN). After all the  
 198 points are classified into the above four categories, the scores can be calculated by their  
 199 corresponding formula in Table 2 (where CN is not used).

200 **Table 2.** List of the categorical skill scores and their formulas.

Name of skill score	Formula	Perfect score	Worst score
Bias Score (BS)	$(H+FA)/(H+M)$	1	0 or N
Probability of Detection (POD)	$H/(H+M)$	1	0
False Alarms Ratio (FAR)	$FA/(H+FA)$	0	1
Threat Score (TS)	$H/(H+M+FA)$	1	0

201

202 In addition to the categorical scores, the Fractions Skill Score (FSS, Roberts and Lean, 2008) is  
 203 also applied to evaluate the model rainfall results, as

204 
$$FSS = 1 - \frac{\frac{1}{N} \sum_{i=1}^N (F_i - O_i)^2}{\frac{1}{N} \sum_{i=1}^N F_i^2 + \frac{1}{N} \sum_{i=1}^N O_i^2}$$
 (1)  
 205



206 where  $N$  is the total number of verification points,  $F_i$  is the forecast value, and  $O_i$  is the observed  
207 value, respectively. The formula shows that a forecast with perfect skill has a FSS of 1, while a  
208 score of 0 means zero skill.

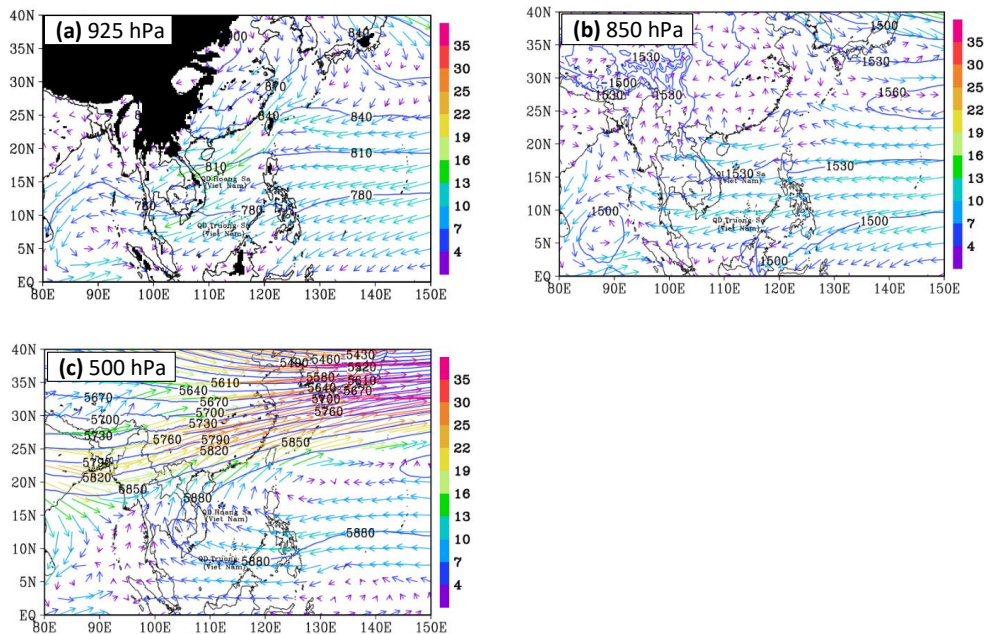
### 209 **3 Overview of the D18 Event**

#### 210 **3.1 Rainfall and its distribution**

211 As introduced earlier, during 8-12 December 2018, an extreme precipitation event occurred in  
212 central Vietnam. The maximum accumulated rainfall was recorded from 9 to 11 December with a  
213 peak daily rainfall greater than 500 mm and 72-h accumulated rainfall exceeds 800 mm (Figs. 1a-d).  
214 Besides, the daily and 72-h rainfalls observed at 69 stations show that the extreme precipitation  
215 occurred along the eastern coastal plains, on the windward side of the Truong Son Range. Especially  
216 over Quang Nam province, where the Truong Son Range reaches its highest of over 2500 m (Figs.  
217 1a-d). In addition, satellite products from the Tropical Rainfall Measuring Mission (TRMM) seriously  
218 underestimates the D18 event (Fig. 1e), but indicates that the rainfall occurred not only in coastal  
219 plains but also over the nearby ocean.

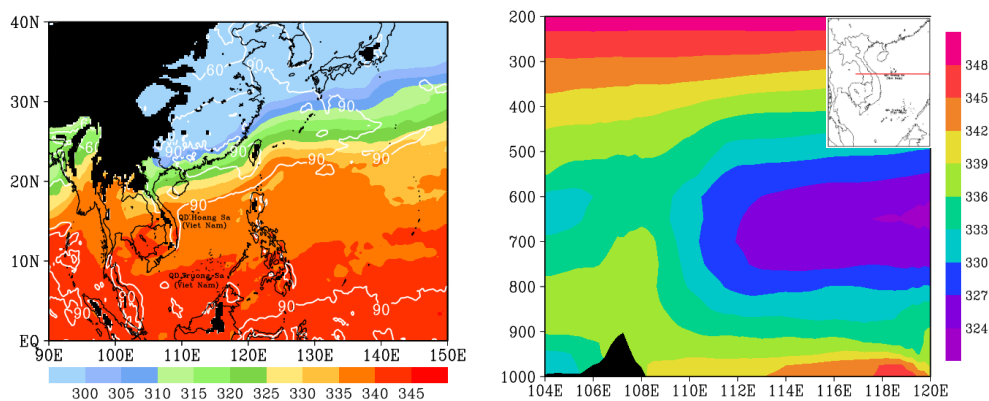
#### 220 **3.2 Synoptic conditions**

221 In this subsection, the synoptic-scale atmospheric conditions during the D18 event are  
222 analyzed. During the D18 event, the horizontal winds at 925 hPa (averaged from 0000 UTC 8 to  
223 1800 UTC 11 December) over central Vietnam and the SCS are characterized by a strong  
224 convergent zone between the northeasterly winds blowing from northeastern China into northern  
225 SCS and central Vietnam, and the easterly winds blowing from the western North Pacific (WNP)  
226 into the SCS (Fig. 4a). The wind speed over northern SCS and central Vietnam is over  $13 \text{ m s}^{-1}$ . At  
227 850 hPa, horizontal winds are predominantly easterly, with speeds of about  $10\text{--}13 \text{ m s}^{-1}$  (Fig. 4b).  
228 At 500 hPa, central Vietnam is affected by southeasterly winds that originated from the easterly  
229 winds over the WNP (Fig. 4c).



230 **Figure 4.** (a) The ERA5 averaged horizontal wind vectors ( $\text{m s}^{-1}$ , color for speed) and geopotential  
231 height (gpm, blue contours, every 30 gpm) at the 925 hPa from 0000 UTC 8 to 1800 UTC 11 Dec  
232 2018. (b) As in (a), but for the 850 hPa. (c) As in (a), but for the 500 hPa. The blacked areas are  
233 where the 925-hPa level is below the ground.

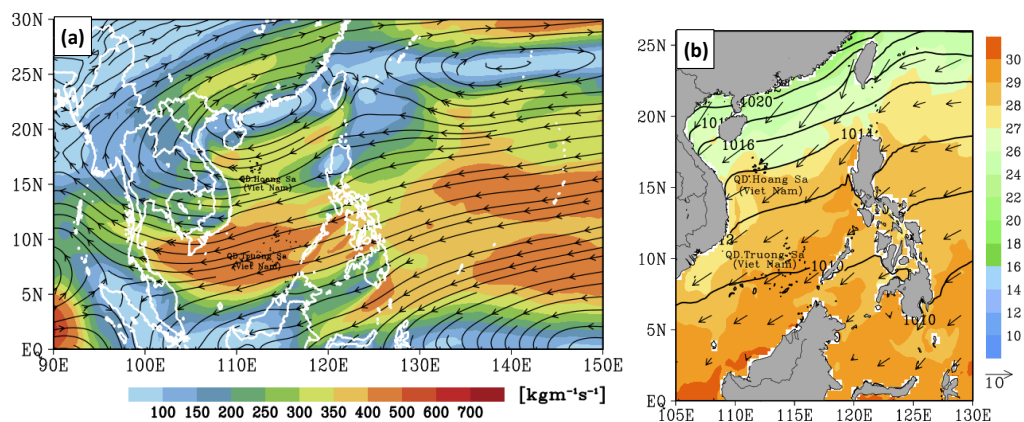
234 From a thermodynamic perspective, the equivalent potential temperature ( $\theta_e$ ) field at 925 hPa  
235 shows that a warm and moist tropical air mass exist in central and SCS with  $\theta_e$  values greater than  
236 335 K, and the relative humidity is around 90 % during the D18 event (Fig. 5a). The high moisture  
237 content combines with a decrease in  $\theta_e$  with altitude, indicating convective instability in the lower  
238 atmosphere below about 500 hPa (Fig. 5b). Furthermore, the interaction between northeasterly and  
239 easterly winds seemed to enhance instability in the lower atmosphere.



240

241 **Figure 5.** (a) The ERA5 averaged equivalent potential temperature (K, color), and relative humidity  
242 (% , white contours, every 30 %) at 925 hPa. The blacked areas are where the 925-hPa level is  
243 below the ground. (b) the east-west vertical cross-section along 16°N (see insert) of averaged  
244 equivalent potential temperature ( $\theta_e$ , K, color, every 5 K), from 0000 UTC 8 to 1800 UTC 11 Dec  
245 2018. The topography is dark shaded.

246 The above analysis suggests that the northeasterly, easterly, and southeasterly winds (cf. Figs.  
247 4a-c) all played an important role in transported unstable air into central Vietnam. Particularly,  
248 when the strong northeasterly and the easterly winds at low levels and southeasterly wind at upper  
249 levels blow into central Vietnam, they bring warm, moist, and unstable air into central Vietnam.  
250 This moisture is transported to central Vietnam by strong moisture flux through the deep column  
251 from the WNP, across the Philippines and the SCS (Fig. 6a). Furthermore, the high SST of the SCS  
252 ( $>27^\circ\text{C}$ ) also help to enhance and maintain abundant moisture during this event (Fig. 6b).



253

254 **Figure 6.** (a) The ERA5 averaged surface–200-hPa vertically integrated moisture flux ( $\text{kg m}^{-1}\text{s}^{-1}$ ).

255 (b) the ERA5 averaged SST ( $^{\circ}\text{C}$ , color), mean sea-level pressure (hPa, isobars, every 2 hPa), and

256 horizontal wind vectors at 10-m height ( $\text{m s}^{-1}$ , vector), from 0000 UTC 8 to 1800 UTC 11 Dec

257 2018.

258 Consequently, the atmospheric conditions and local topographic characteristics in interaction

259 result in moisture convergence and forced uplift in the lower troposphere during the D18 event.

260 This can be seen in Fig. 7, where extensive rising motion occurs in the lower troposphere along

261 coastal Vietnam, with a maximum value of  $-1.2 \text{ Pa s}^{-1}$ . Besides, Figs. 7a,b also indicate that the

262 strong northeasterly wind along with warm, moist and unstable air is blocked by the Truong Son

263 Range. This pattern suggests that the Truong Son Range also played an important role in the

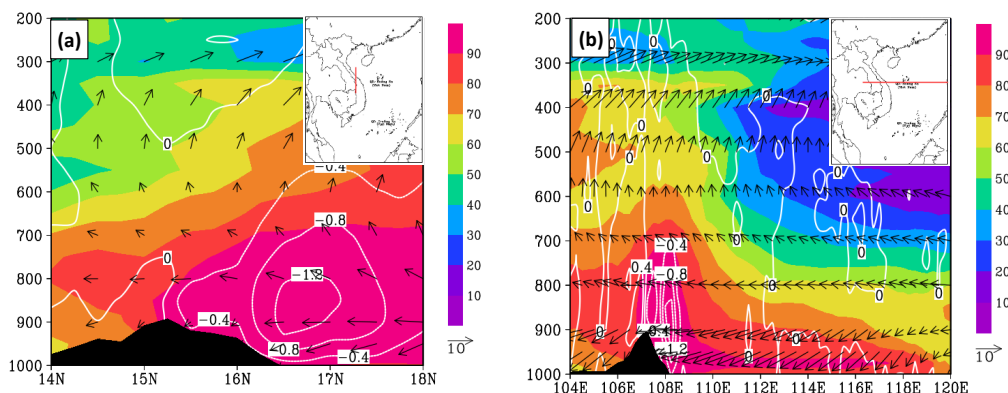
264 development of heavy rainfall in central Vietnam in D18. In detail, when the northeasterly and

265 easterly winds at low levels blow into central Vietnam and become block by the Truong Son Range,

266 which is located along the border of Vietnam and Laos, forced uplift is resulted at the windward

267 side, with downward motion over the lee side (in Laos, Fig. 7b).

268

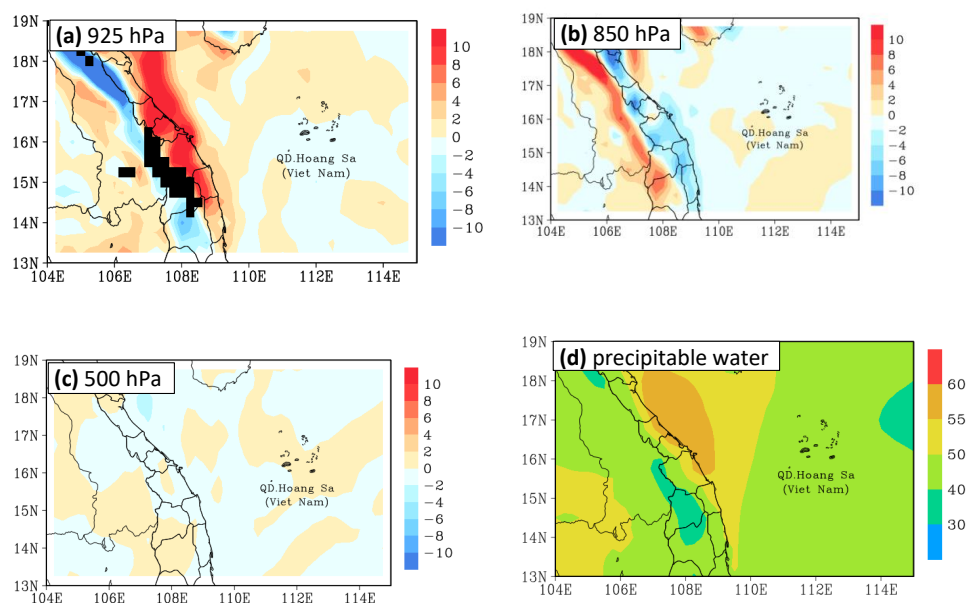


269 **Figure 7.** (a) The ERA5 the south-north vertical cross-section along 107.5°E (see insert) of  
270 averaged horizontal wind ( $\text{m s}^{-1}$ , vectors) and vertical motions ( $\text{Pa s}^{-1}$ ; white contours, negative for  
271 upward motion), and relative humidity (%), shaded), from 0000 UTC 8 to 1800 UTC 11 Dec 2018.  
272 The topography is dark shaded. (b) As in (a), but for the vertical cross-section along 16° N.

273 As described above, when the strong northeasterly and easterly winds at low levels blow into  
274 central Vietnam, they bring warm, moist, and unstable air that originated in the WNP and is  
275 enhanced over the SCS. Then, this air is blocked by the Truong Son Range, which has a height of  
276 around 2 km, leading to forced convergence and upward motion at low levels and divergence  
277 further above. These conditions consequently lead to moisture flux convergence of over  $8 \times 10^{-4} \text{ g}$   
278  $\text{kg}^{-1} \text{ s}^{-1}$  at 925 hPa (Fig. 8a) and moisture flux divergence at 850 hPa with comparable magnitudes  
279 (Fig. 8b). This divergence reduces sharply further up toward the middle and upper levels (Fig. 8c).  
280 These factors create a moist atmosphere with a precipitable water amount (through the deep  
281 column) exceeding 50 mm during the D18 event (Fig. 8d). The above atmospheric ingredients and  
282 characteristics in local topography in combination created favorable environmental conditions to  
283 trigger orographic rainfall. As a consequence, the D18 event happened.

284





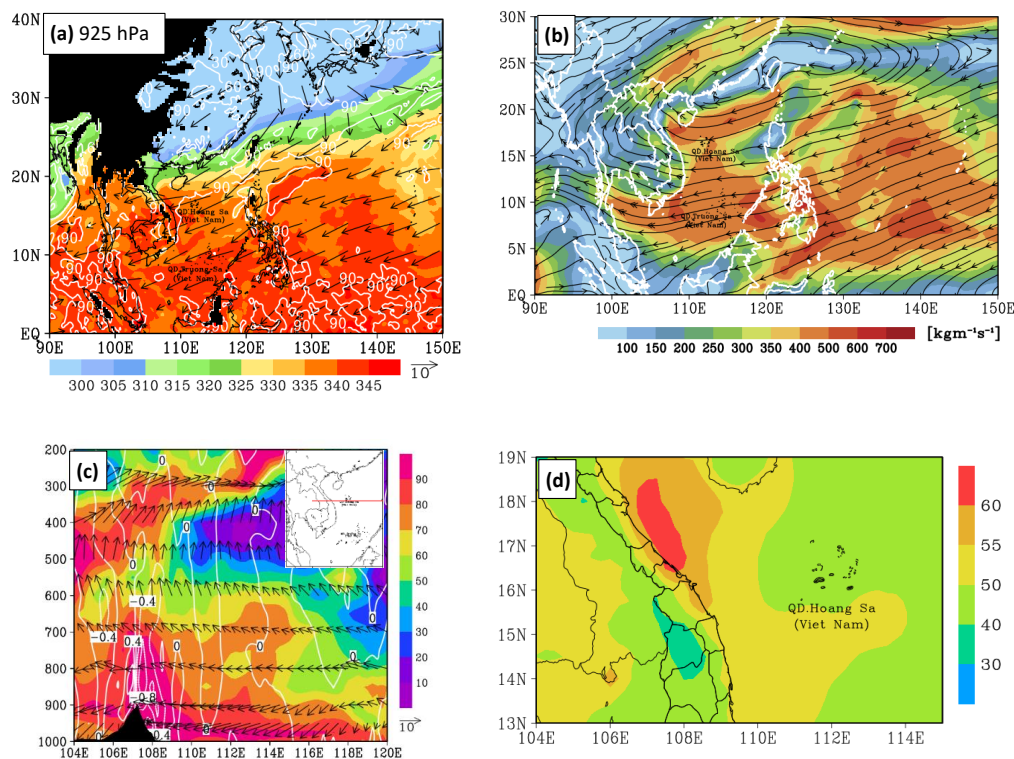
285 **Figure 8.** (a) The ERA5 averaged moisture convergence/ divergence ( $\times 10^{-4}$ ,  $\text{g kg}^{-1} \text{s}^{-1}$ , shaded,  
286 positive for convergence) at the 925 hPa, from 0000 UTC 8 to 1800 UTC 11 Dec 2018. The blacked  
287 areas are where the 925-hPa level is below the ground. (b) As in (a), but for the 850 hPa. (c) As in  
288 (a), but for the 500 hPa. (d) The ERA5 averaged precipitable water between surface and 200 hPa  
289 (mm), from 0000 UTC 8 to 1800 UTC 11 Dec 2018.

### 290 3.3 Evolution of precipitating clouds

291 In this part, the local thermodynamic conditions that led to the D18 event are analyzed. Figure  
292 8 shows these conditions at 1200 UTC 8 December 2018. At this time, it is quite warm and moist  
293 over central Vietnam and the SCS, with  $\theta_e$  of at least 335 K (Fig. 9a). As mentioned, this moisture  
294 is transported to central Vietnam from the WNP by the strong moisture flux, across the Philippines  
295 and the SCS and eventually intercepted by the Truong Son Range at the western border of Vietnam  
296 (Figs. 9b,c). The thermodynamic conditions and local orography in interaction lead to a moist  
297 atmosphere with a precipitable water amount exceeding 50 mm (Fig. 9d). Furthermore, the vertical  
298 wind profile also indicates both warm advection at low levels (veering winds with height) and a



299 considerable southerly wind shear between 950 and 500 hPa (Fig. 9c). These thermodynamic  
300 conditions were favorable for the development of convection and precipitation.



301 **Figure 9.** (a) The ERA5  $\theta_e$  (K, shaded), horizontal winds ( $\text{m s}^{-1}$ , vector), and relative humidity (%,  
302 white contours, every 30 gpm) at 925 hPa. The blacked areas are where the 925-hPa level is below  
303 the ground. (b) Surface–200-hPa vertically integrated moisture flux ( $\text{kg m}^{-1} \text{s}^{-1}$ ). (c) East-west vertical cross-  
304 section along  $16^\circ\text{N}$  (see insert) of vertical motions ( $\text{Pa s}^{-1}$ , white contours), relative humidity (%,  
305 shaded), and horizontal winds ( $\text{m s}^{-1}$ , vector). The topography is black shaded. (d) Precipitable  
306 water between surface and 200 hPa (mm). All panels are for 1200 UTC 8 Dec 2018.

307 On satellite imageries from 1200 UTC 8 to 1100 UTC 9 December (Fig. S1), a series of deep  
308 convective clouds (cumulonimbi, or Cb) first form over northern and central Vietnam and Laos on 8  
309 December, with mainly a northeast-southwest to east-west alignment. With blackbody temperatures

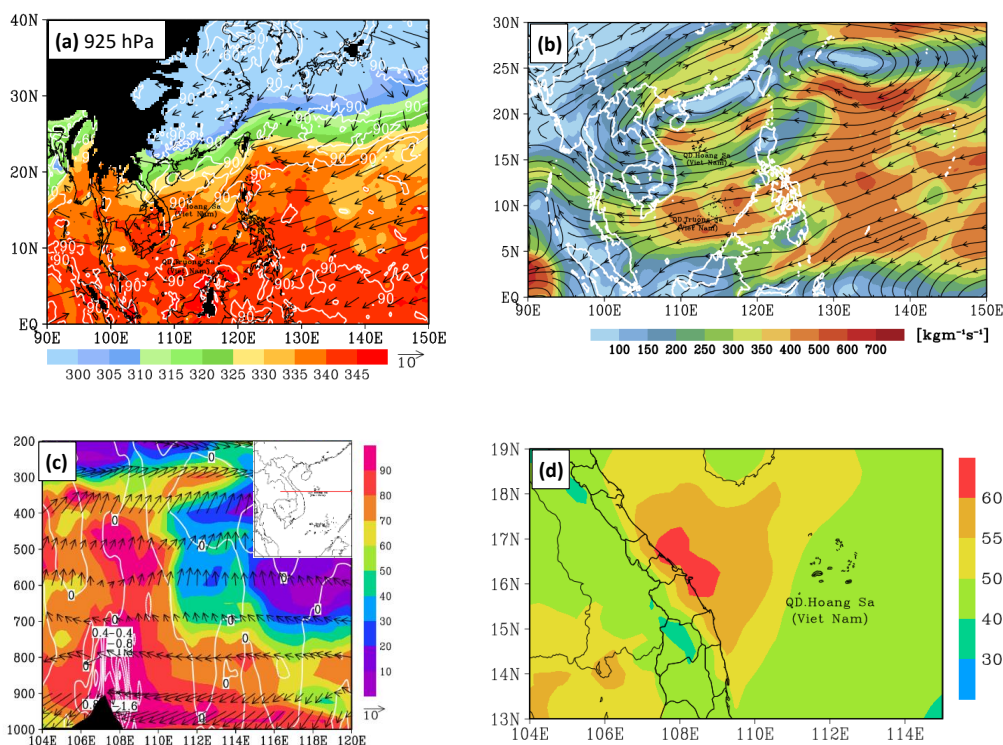


310 ( $T_B$ ) below  $-42^\circ\text{C}$ , several isolated deep cells also develop near the coast over the southern part of  
311 the study area after 0200 UTC on 9 December (Fig. S1). Generally, these deep Cb clouds tend to  
312 move slowly offshore and weaken after a few hours. Meanwhile, the study area is also covered by  
313 precipitating clouds known as nimbostratus (Ns) that are not as deep, with cloud-top  $T_B$  at  $-20^\circ\text{--}0^\circ$   
314 C and above (Fig. S1). These Ns clouds first form over the northern part of the study area and then  
315 grow and expand southward along the coast, eventually cover the entire study area on 9 December  
316 (Fig. S1). As analyzed above, both deep Cb clouds and the persistent Ns clouds produced long-  
317 lasting rainfall for hours, starting along the coast from 1200 to 1700 UTC 8 December. After that,  
318 the rain area extends both inland and over the coastal sea (Fig. S2). The rainfall intensity is the  
319 greatest from 2000 UTC 8 to 0200 UTC 9 December, with a column-maximum radar reflectivity  
320 ( $C_{\max}$ )  $\approx 40$  dBZ (Fig. S2). Afterwards, the rainfall intensity decreases to some extent but remain at  
321 15-35 dBZ rather steadily (Fig. S2). While the precipitation is not too intense, it falls persistently  
322 over many hours, leading to high 24-h rainfall accumulation at some locations. Thus, the local  
323 thermodynamic conditions seem to maintain for many hours and lead to the continuous  
324 development of precipitating clouds during much of 8 December.

325 At 1200 UTC 9 December, a warm and moist atmospheric is still maintained over central  
326 Vietnam and the SCS, with  $\theta_e > 335$  K (Fig. 10a). The moisture continued to be transported from  
327 the east, with the northeasterly wind played the main role in this transport (Fig. 10b). These  
328 moisture conditions are associated with the northeasterly wind over central Vietnam seemed  
329 stronger than the previous day, leading to a stronger low-level uplifting than that on 8 December  
330 (Fig. 10c). Consequently, the atmosphere becomes moister with increases precipitable water amount  
331 to over 55 mm (Fig. 10d). These thermodynamic conditions played a role to sustain the  
332 development of precipitating clouds on 9 December. On this day (since 1200 UTC), satellite  
333 imageries also show some characteristics of deep convection over the coastal area (Fig. S3), but the  
334 cloud top temperatures, in general, are not as cold as on 8 December. Meanwhile, the lower



335 precipitating Ns clouds cover much of the study area from 1200 UTC 9 to 0300 UTC 10 December,  
336 then gradually disintegrate (Fig. S3). These clouds kept producing rainfall for the whole day, with  
337 the higher  $C_{\max}$  values ( $\sim 40$  dBZ) and rainfall intensity from 1200 UTC 9 to around 0000 UTC 10  
338 December (Fig. S4), mainly over the coastal plain and nearby sea. After that, the rain gradually  
339 decreases in both intensity and areal coverage.

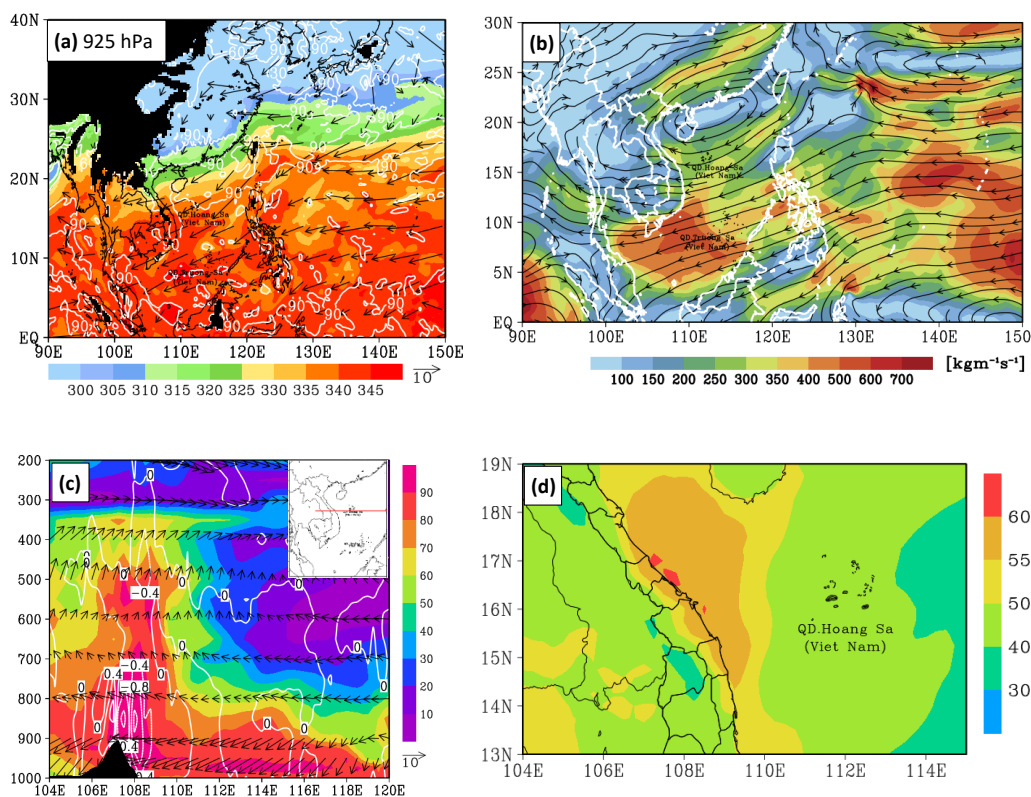


340 **Figure 10.** As in Fig. 9, except for 1200 UTC 9 Dec 2018.

341 At 1200 UTC 10 December, the atmosphere remains very moist with a precipitable water  
342 amount of 55 mm (Fig. 11d). Some of the local dynamical and thermodynamically parameters,  
343 however, are reduced from one day earlier and become not as favorable, including the upward  
344 motion over central Vietnam (Fig. 11c) and moisture flux (Fig. 11b). Hence, the development of  
345 precipitating clouds also reduces significantly on this day and mostly exist offshore over the ocean



346 (Fig. S5). Compared to the past two days, the development of convective cells is also reduced. Near  
347 the coast, only three convective cells developed on 10 December, one at 1400 UTC, the second at  
348 2000 UTC, and the third one shortly after 2200 UTC. Also, moving eastward and offshore after  
349 formation, these relatively small cells spend only 1-3 h over land. In general, the environmental  
350 conditions become less favorable for developing rain clouds after 1200 UTC 10 December.  
351 Consequently, there is a significant decrease in rainfall, which occurs mainly during 1200-1600  
352 UTC then weaken with time (Fig. S6).



353 **Figure 11.** As in Fig. 9, except for 1200 UTC 10 Dec 2018.

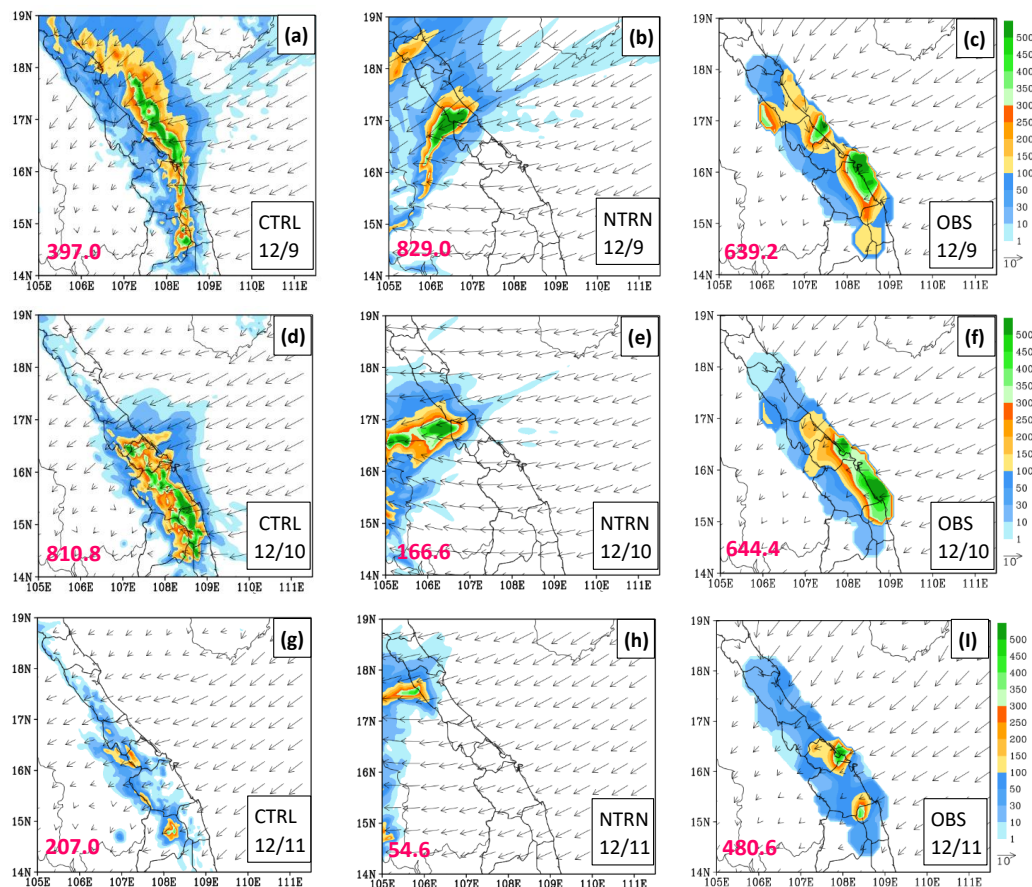
354 **4 Model Simulation Results**



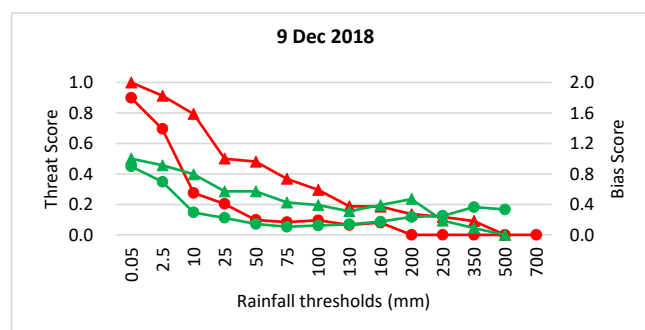
355 In this section, the model simulation results are used to investigate the role of topography in  
356 the development of clouds and rainfall in the D18 event, and the CReSS model is also evaluated for  
357 its ability to reproduce the event over the study area.

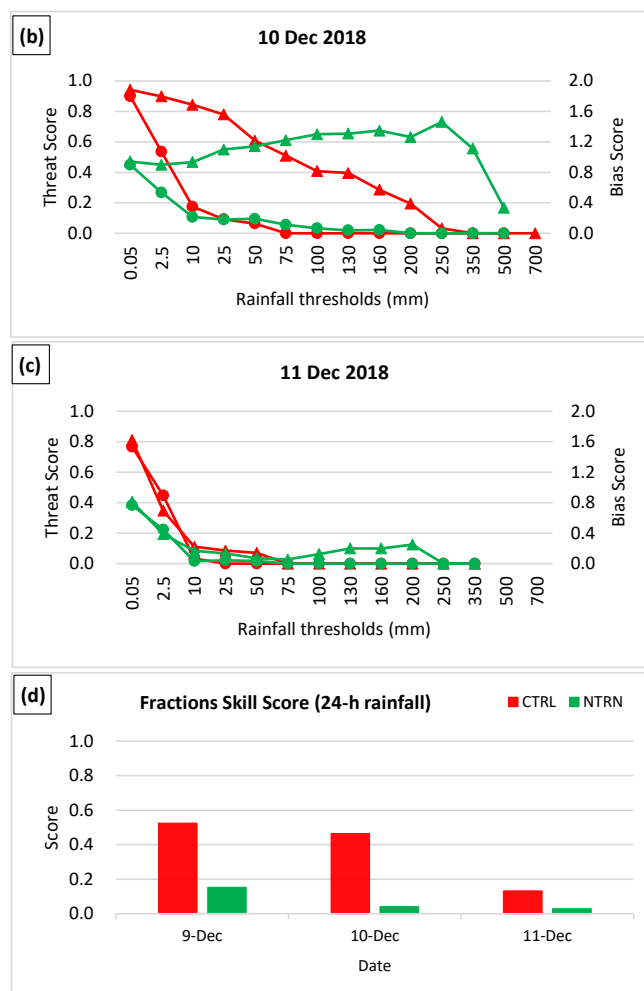
358 Figure 12 presents the daily averaged surface horizontal winds and daily rainfall in CTRL and  
359 NTRN for each of the three days from 9 to 11 December 2018. In CTRL, the model produces a  
360 maximum 24-h rainfall of around 400 mm on 9 December (Fig. 12a), roughly comparable in  
361 magnitude to the observation (Fig. 12c). While one should bear in mind that the limited number of  
362 rain gauges have a smaller coverage area and cannot resolve the detailed distribution of rainfall (cf.  
363 Fig. 2b), the model rainfall in CTRL is slightly more offshore north of  $16^{\circ}$  N but more inland near  
364  $16^{\circ}$  N, thus is not as abundant along the coast compared to the observation. In other words, model  
365 rainfall has some location errors but the magnitude is comparable by visual inspection. For surface  
366 winds, their direction and magnitude are well simulated by the CTRL experiment (Fig. 12).

367 An objective and more quantitative verification of model rainfall can be provided by the threat  
368 score (TS) computed at the rain-gauge sites, which shows that the model has high score at low  
369 thresholds of  $\leq 10$  mm (per 24 h) but gradually decreases toward higher thresholds (Fig. 13a, red  
370 curve). In particular, the TS is about 0.5 at 25-50 mm, below 0.2 above 160 mm, and about 0.1 at  
371 350 mm. Eventually, the TS drops to zero at 500 mm, which is not too far from the observed peak  
372 rainfall of over 500 mm (at Da Nang, cf. Fig. 1a). The bias score (BS) confirms that the model does  
373 not produce enough rainfall over the coastal plains, as its value drops from about 1.0 at 0.05 mm to  
374 below 0.4 at and above 250 mm. As another objective measure of overall quality of prediction, the  
375 fraction skill score (FSS) is about 0.5 for 9 December. Overall, the model appears to produce too  
376 much rainfall offshore north of  $16^{\circ}$  N and not enough rainfall along the coast, and this might be to  
377 some extent linked to its surface wind coming more from the east-northeast, compared to northeast  
378 in the ERA5 analysis (Figs. 12a,c), leading to somewhat different locations of low-level  
379 convergence of wind and moisture.



380 **Figure 12.** Simulated daily-mean surface horizontal wind vectors ( $\text{m s}^{-1}$ , reference length at right  
 381 column) and 24-h accumulated rainfall (mm, color) in CTRL (left column) and NTRN (middle  
 382 column), and the observed rainfall at gauge sites (OBS), overlaid with the daily-mean surface wind  
 383 vectors derived from the ERA5 data (right column). From top to down are: (a-c) 9 Dec, (d-f) 10  
 384 Dec, and (g-i) 11 Dec 2018. The pink number at the lower left indicates the maximum value of 24-h  
 385 rainfall.





386 **Figure 13.** (a)-(c) The threat scores (red) and bias scores (green) of 24-h accumulated rainfall for  
387 the CTRL (curve with triangles) and NTRN (curve with dots) experiments for the three days of 9-11  
388 Dec 2018. (d) Fractions skill scores of 24-h accumulated rainfall for the two experiments.

389 For 10 December, while similar differences in prevailing surface winds still exist between  
390 model simulation and ERA5 data, the model rainfall location has improved with better agreement  
391 with the observation (Figs. 12d,f), but in general slightly more inland and not right on the coast.  
392 Both over 600 mm, the observed and simulated peak daily rainfall values are again comparable.





393 Due to the improvement in spatial pattern, the TSs exhibit higher values than those for the previous  
394 day across low to middle thresholds (up to 200 mm) but reduce to zero at 250 mm (Fig. 13b), while  
395 the FSS (near 0.46) is only slightly reduced (Fig. 13d). In agreement with the better TS values, the  
396 BS remains between 0.8 and about 1.4 from low thresholds up to 350 mm, and drops to about 0.35  
397 at 500 mm (Fig. 13b).

398 For 11 December, the model does not simulate well the rainfall field, as its rainfall is displaced  
399 toward the Truong Son Range (and the border to Laos), instead of over the coastal plain as observed  
400 (Figs. 12g,i). The spatial coverage of model rainfall is smaller and the peak amount (~200 mm) also  
401 lower compared to the rain-gauge data, while the surface wind appears weaker than the ERA5 data  
402 as well. While the observed peak amount became lower as the D18 event was coming to an end, the  
403 TSs also decrease rapid with threshold, and are close to 0.1 at just 10 mm and become zero at and  
404 above 70 mm (Fig. 13c). Consistent with the inadequate amount over land, the BSs also decrease  
405 rapidly with thresholds, from about 0.8 at 0.05 mm to below 0.3 over 100-200 mm. For this day, the  
406 FSS is only about 0.14 and significantly lower than the values for 9 and 10 December (Fig. 13d).  
407 Likely also related to the weaker surface winds in the model, the less-than-ideal results of rainfall  
408 may be also affected by the longer range of integration, at 66-90 h, for 11 December.

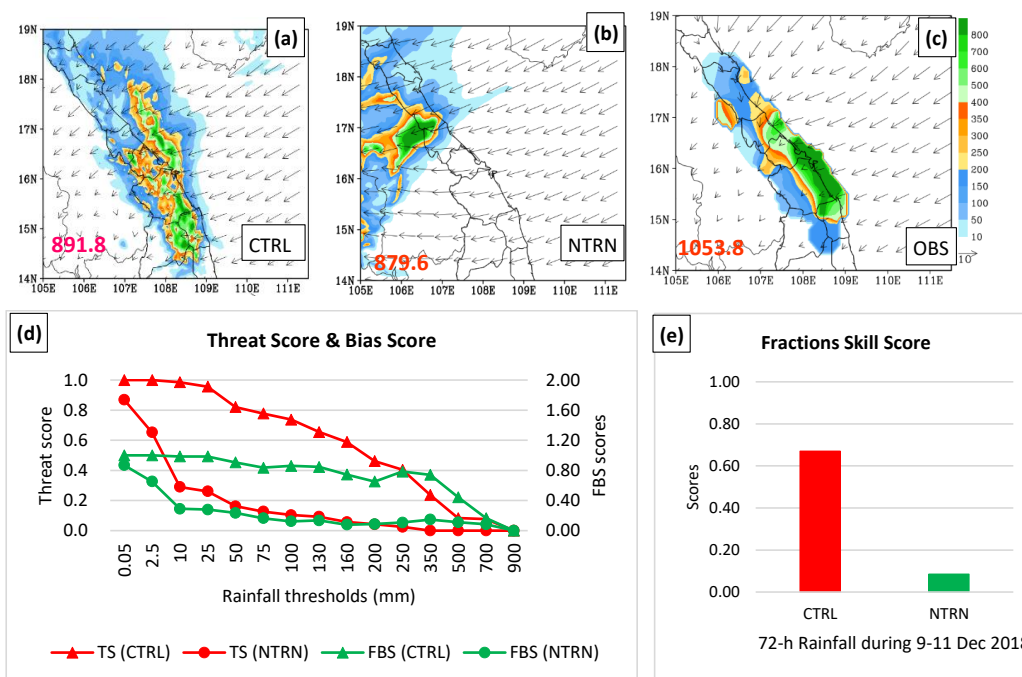
409 To test the impact of topography in the D18 event, the NTRN experiment was carried out.  
410 Without the terrain, the rainfall as simulated by CReSS would be displaced much more inland from  
411 the coastal region for all three days of 9-11 December (Figs. 12b,e,h), and more importantly, the  
412 pattern would no longer be elongated and parallel to the coast, even though the peak amounts are  
413 similar to the observation. Thus, the topography was fundamental in determining the basic rainfall  
414 area and pattern in the D18 event. With incorrect distributions, the TS values (Fig. 13, green curves)  
415 are much lower and drop to below 0.2 at thresholds above 10-25 mm for all three days. The  
416 thresholds at which the TSs decrease to zero are 200, 75, and 25, respectively for the three days, and  
417 much lower than those in the CTRL, especially for 9 and 10 December. The BS values in the NTRN



418 also tend to be lower than those in the CTRL, sometimes much lower, reflecting its incorrect  
419 location and thus little rainfall at gauge sites with rainfall in reality. The FSS values are also much  
420 lower, with values near 0.16, 0.04, and 0.04 for the three days. Without the topography, the surface  
421 wind pattern near the coast and over land would be much stronger and very different, due to the  
422 lack of its blocking and uplifting effects, and also the associated thermodynamic effects.

423 For the D18 event as a whole, the three-day total rainfall distribution produced by the model  
424 compares quite favorably with the observation in both quantity and spatial pattern (Figs. 14a,c),  
425 with generally minor displacement errors more toward inland at around 15°-16° N. Despite these  
426 errors, the spatial distribution of rainfall in the model corresponds well to the zone of low-level  
427 moisture convergence in the ERA5 analysis (Fig. 8a). In agreement with visual assessment, the TSs  
428 of the 72-h QPFs are quite high across even heavy-rainfall thresholds: around 0.8 at 100 mm (per 72  
429 h), close to 0.5 at 200 mm, above 0.2 at 350 mm, and 0.1 at 700 mm, with an overall FSS  $\approx$  0.7  
430 (Figs. 14d,e). As shown, the rainfall fields for individual days in D18 are very different without the  
431 topography in NTRN, and the same is true for the whole event (Fig. 14b). The TSs also indicate a  
432 much lower skill in QPF, with TS below 0.2 at  $\geq$  50 mm (per 72 h) and TS = 0 at  $\geq$  350 mm, BS  
433 below 0.35 at  $\geq$  10 mm, and also an overall FSS of less than 0.1 (Figs. 14d,e). The results in Figs.  
434 12 and 14 also indicate a significant wind-blocking effect by the Truong Son Range. In CTRL, the  
435 surface northeasterly winds commonly exceed 10 m s<sup>-1</sup> in speed over the SCS, but are reduced  
436 significantly (and even to near-zero speed) near the Annamite Range (and in Laos). On the contrary,  
437 there is no reduction in speed as the winds blow across central Vietnam in NTRN, without the  
438 blocking effect of the topography.

439



440 **Figure 14.** (a)-(c) As in Figs. 11a-c, except for three-day averaged surface horizontal wind vectors  
 441 and 72-h accumulated rainfall over 9-11 Dec 2018. (d), (e) As in Figs. 12c,d, except for TSs and  
 442 FSSs of the 72-h accumulated rainfall over 9-11 Dec 2018.

## 443 5 Conclusion

444 In this study, the extreme precipitation event that occurred on 8-12 December 2018 along the  
 445 coast of central Vietnam is analyzed, and the simulation results by a CRM (the CReSS model) is  
 446 evaluated. The major findings are summarized below.

447 Analysis on the D18 event has revealed several key factors which led to this record-breaking  
 448 rainfall event: First, for all four days from 8 to 11 December, the strong northeasterly winds in the  
 449 lower troposphere blew from the Yellow Sea into the SCS, and interacted with strong low-level  
 450 easterly winds (below 700 hPa) over the SCS. This interaction strengthened the upstream easterly to  
 451 northeasterly winds and generated strong low-level convergence, as the winds blew into central  
 452 Vietnam and was blocked by the Truong Son Range, resulting in forced uplift near the surface over



453 the coastal plains. Consequently, heavy rainfall was produced along the coast of central Vietnam.  
454 Second, the strong easterly winds played an important role in transporting moisture from the WNP,  
455 across the Philippines and the SCS, into central Vietnam. Third, the Truong Son Range also played  
456 an important role in this event due to its barrier effect. Finally, the high SST of the SCS ( $>27^{\circ}\text{C}$ )  
457 also acted to help replenishing the moisture in this event. This above mechanism in the D18 event is  
458 different from those documented in previous studies. Particularly, according to previous studies, the  
459 heavy and extreme rainfall events are usually due to the multi-interaction between the northeasterly  
460 wind and preexisting tropical disturbance over the SCS and local topography or tropical cyclone or  
461 impacts by ENSO or MJO. However, these factors have not appeared during the D18 event.  
462 Therefore, we suggest that the interaction of the northeasterly and easterly winds in the moist,  
463 unstable atmospheric and local topography can also lead to heavy precipitation events along the  
464 central coastal plains of Vietnam. Another interesting finding of this study is that even though short  
465 periods of heavy rainfall from deep convection also contributed, the extreme rainfall of the D18  
466 event was mainly from the persistent rain from nimbostratus clouds (Ns) that do not possess a high  
467 reflectivity or a very cold cloud top.

468 The evaluation of model simulation results at a grid size of 2.5 km indicates the following. In  
469 the CTRL, the CReSS model has reproduced this event's rainfall field quite well, for both daily and  
470 three-day accumulations, but with some displacement errors. In terms of objective verification skill  
471 scores, in particular, CReSS displays high skills at heavy-rainfall thresholds for both daily rainfall  
472 ( $\text{TS} \geq 0.1$  at 200-350 mm and  $\text{FSS} \approx 0.5$  for 9 and 10 December) and 72-h total ( $\text{TS} \approx 0.1$  at 700  
473 mm and  $\text{FSS} \approx 0.7$ ). However, the rainfall simulation is less ideal for 11 December (TS drops to  
474 zero at thresholds  $\geq 75$  mm), which had less rainfall and is at a longer range (than the previous two  
475 days). In the sensitivity test of NTRN where the topography is removed, the model produced a  
476 different rainfall pattern not along the coast as observed (and in CTRL), thus confirming the  
477 important role by the Truong Son Range in this event. In addition, the evaluation of simulation



478 results also shows that the CReSS model has well simulated the surface winds, both in their  
479 direction and magnitude.

480 The above result also shows the promising capacity of the CReSS model for research and  
481 forecast of heavy rainfall in Vietnam. In a follow-up paper, a set of high-resolution time-lagged  
482 ensemble prediction is performed using the CReSS model, and the predictability of the D18 event  
483 will be evaluated.

#### 484 **Code and data availability**

485 The CReSS model used in this study and its user's guide are available at the model website at  
486 [http://www.rain.hyarc.nagoyau.ac.jp/~tsuboki/cress\\_html/index\\_cress\\_eng.html](http://www.rain.hyarc.nagoyau.ac.jp/~tsuboki/cress_html/index_cress_eng.html).

#### 487 **Author contribution**

488 Duc Van Nguyen prepared datasets, executed the model experiments, performed analysis, and  
489 prepared the first draft of the manuscript. Chung-Chieh Wang provided the funding, guidance and  
490 suggestions during the study, and participated in the revision of the manuscript.

#### 491 **Competing interests**

492 The authors declare that they have no conflict of interest.

493 **Acknowledgement.** We thank Mr. Nguyen Tien Toan at Mid-central Regional Hydro-  
494 Meteorological Centre, Viet Nam for kindly providing the observed rainfall and radar data, as well  
495 as his comment. We acknowledge the free use of ECMWF ERA5 from Copernicus Climate Change  
496 Service (C3S) Climate Data Store (CDS) [https://www.ecmwf.int/en/forecasts/datasets/reanalysis-](https://www.ecmwf.int/en/forecasts/datasets/reanalysis-datasets/era5)  
497 [datasets/era5](https://www.ecmwf.int/en/forecasts/datasets/reanalysis-datasets/era5). The Vietnam Gridded Precipitation rainfall dataset is available at  
498 <http://danida.vnu.edu.vn/cpis/en/content/gridded-precipitation-data-of-vietnam.html>. The TRMM  
499 3B42 satellite data are from [https://disc.gsfc.nasa.gov/datasets/TRMM\\_3B42\\_7/summary](https://disc.gsfc.nasa.gov/datasets/TRMM_3B42_7/summary). The IR1  
500 Himawari imagines data are from Central Weather Bureau, Taiwan at <https://www.cwb.gov.tw>.



501 **References**

- 502 Akter, N., and Tsuboki, K.: Characteristics of Supercells in the Rainband of Numerically Simulated  
503 Cyclone Sidr., SOLA, 6A, 025–028. <https://doi.org/10.2151/sola.6A-007>, 2010.
- 504 Akter, N., and Tsuboki, K.: Numerical Simulation of Cyclone Sidr Using a Cloud-Resolving Model:  
505 Characteristics and Formation Process of an Outer Rainband. *Mon. Wea. Rev.*, 140, 789-810.  
506 <http://dx.doi.org/10.1175/2011MWR3643.1>, 2012.
- 507 Bui, M.T.: Extratropical forcing of submonthly variations of rainfall in Vietnam, *J. Climate*, 32 (8),  
508 2329-2348, 2019.
- 509 Chen, T.-C., Tsay, J.-D., Yen, M.-C., and Matsumoto, J.: Interannual variation of the late fall rainfall  
510 in central Vietnam, *J. Climate*, 25, 392–413, 2012.
- 511 Cotton, W.R., Tripoli, G.J., Rauber, R.M., and Mulvihill, E.A.: Numerical simulation of the effects  
512 of varying ice crystal nucleation rates and aggregation processes on orographic snowfall. *J.*  
513 *Climate Appl. Meteorol.* 25, 1658–1680, 1986.
- 514 Huffman, G.J., D.T. Bolvin, E.J. Nelkin, and R.F. Adler.: TRMM (TMPA) Precipitation L3 1 day  
515 0.25 degree x 0.25 degree V7, Edited by Andrey Savtchenko, Goddard Earth Sciences Data and  
516 Information Services Center (GES DISC), Accessed on 10-12-2019,  
517 10.5067/TRMM/TMPA/DAY/7, 2016.
- 518 Hersbach, H., Bell, B., Berrisford, P., Biavati, G., Horányi, A., Muñoz Sabater, J., Nicolas, J., Peubey,  
519 C., Radu, R., Rozum, I., Schepers, D., Simmons, A., Soci, C., Dee, D., and Thépaut, J.-N.: ERA5  
520 hourly data on pressure levels from 1979 to present. Copernicus Climate Change Service (C3S)  
521 Climate Data Store (CDS). (Accessed on 14-06-2021). Doi: 10.24381/cds.bd0915c6, 2018b.
- 522 Hersbach, H., Bell, B., Berrisford, P., Biavati, G., Horányi, A., Muñoz Sabater, J., Nicolas, J., Peubey,  
523 C., Radu, R., Rozum, I., Schepers, D., Simmons, A., Soci, C., Dee, D., and Thépaut, J.-N.: ERA5



- 524 hourly data on single levels from 1979 to present. Copernicus Climate Change Service (C3S)  
525 Climate Data Store (CDS). (Accessed on 14-06-2021). DOI: 10.24381/cds.adbb2d47, 2018a.
- 526 Ikawa, M., and Saito, K.: Description of a non-hydrostatic model developed at the Forecast Research  
527 Department of the MRI, MRI Technical report 28, Japan Meteorological Agency, Tsukuba,  
528 Japan, 1991.
- 529 Lin, Y.-L., Farley, R.D., and Orville, H.D.: Bulk parameterization of the snow field in a cloud model.  
530 *J. Climate Appl. Meteorol.* 22, 1065–1092, 1983.
- 531 Murakami, M.: Numerical modeling of dynamical and microphysical evolution of an isolated  
532 convective cloud – the 19 July 1981 CCOPE cloud, *J. Meteorol. Soc. Jpn.*, 68, 107–128, 1990.
- 533 Murakami, M., Clark, T.L., and Hall, W.D.: Numerical simulations of convective snow clouds over  
534 the Sea of Japan: Two-dimensional simulation of mixed layer development and convective  
535 snow cloud formation, *J. Meteorol. Soc. Jpn.* 72, 43–62, 1994.
- 536 Nguyen-Le, D., and Matsumoto, J.: Delayed withdrawal of the autumn rainy season over central  
537 Vietnam in recent decades. *Int. J. Climatol.*, 36, 3002–3019, 2016.
- 538 Nguyen-Thi, H.A., Matsumoto, J., Ngo-Duc, T., and Endo, N.: Long-term trends in tropical cyclone  
539 rainfall in Vietnam. *J. Agrofor. Environ.*, 6(2), 89–92, 2012.
- 540 Nguyen-Xuan, T., Ngo-Duc, T., Kamimera, H., Trinh-Tuan, L., Matsumoto, J., Inoue, T., and Phan-  
541 Van, T.: The Vietnam Gridded Precipitation (VnGP) Dataset: Construction and validation.  
542 *SOLA*, 12, 291–296, <https://doi.org/10.2151/sola.2016-057>, 2016.
- 543 Ohigashi, T., and Tsuboki, K.: Shift and intensification processes of the Japan-Sea Polar-Airmass  
544 Convergence Zone associated with the passage of a mid-tropospheric cold core. *Journal of the  
545 Meteorological Society of Japan*, 85(5), 633–662, 2007.



- 546 Roberts, N.M., and Lean, H.W.: Scale-selective verification of rainfall accumulations from high-  
547 resolution forecasts of convective events. *Mon. Wea. Rev.*, 136, 78–97, 2008.
- 548 Tran, T., Coauthors: The Climate Change and Sea Level Rise Scenarios for Viet Nam. The Ministry  
549 of Natural Resources and Environment. Page count:170, 2016.
- 550 Tsuboki, K., and Sakakibara, A.: Large-Scale Parallel Computing of Cloud Resolving Storm  
551 Simulator. In: Zima H.P., Joe K., Sato M., Seo Y., Shimasaki M. (eds) High Performance  
552 Computing. ISHPC 2002. Lecture Notes in Computer Science. Springer, Berlin, Heidelberg.  
553 Vol 2327, [https://doi.org/10.1007/3-540-47847-7\\_21](https://doi.org/10.1007/3-540-47847-7_21), 2002.
- 554 Tsuboki, K., and Sakakibara, A.: CReSS User's Guide (17th IHP training course text). Page count:  
555 273, 2007.
- 556 Takahashi, H.G., Yoshikane, T., Hara, M., and Yasunari, T.: High-resolution regional climate  
557 simulations of the longterm decrease in September rainfall over Indochina. *Atmos. Sci. Let.*, 10,  
558 14–18, doi:10.1002/asl.203, 2009.
- 559 Vu, V.T., Nguyen, T.H., Nguyen, V.T., Nguyen, V.H., Pham, T.T.H., and Nguyen, T.L.: Effects of  
560 ENSO on Autumn Rainfall in Central Vietnam. *Advances in Meteorology*, Vol. 2015, Article  
561 ID 264373, 12 pages. <http://dx.doi.org/10.1155/2015/264373>, 2015.
- 562 van der Linden, R., Fink, A.H., Phan-Van, T., and Trinh-Tuan, L.: Synoptic-dynamic analysis of early  
563 dry-season rainfall events in the Vietnamese central highlands. *Mon. Wea. Rev.*, 144, 1509–  
564 1527. <https://doi.org/10.1175/MWR-D-15-0265.1>, 2016.
- 565 Wilks, D.S.: *Statistical Methods in the Atmospheric Sciences*, Academic Press. Page count: 648.
- 566 Wang, C.-C., Lin, B.-X., Chen, C.-T., Lo, S.-H., 2015. Quantifying the effects of long-term climate  
567 change on tropical cyclone rainfall using cloud-resolving models: Examples of two landfall  
568 typhoons in Taiwan, *J. Climate*, 28, 66-85. <https://doi.org/10.1175/JCLI-D-14-00044.1>, 2006.





- 569 Wu, P., Fukutomi, Y., and Matsumoto, J.: The impact of intraseasonal oscillations in the tropical  
570 atmosphere on the formation of extreme central Vietnam precipitation. SOLA, 8, 57–60.  
571 <https://doi.org/10.2151/sola.2012-015>, 2012.
- 572 Wang, C. G., Liang, J., and Hodges, K. I.: Projections of tropical cyclones affecting Vietnam under  
573 climate change: Downscaled HadGEM2-ES using PRECIS 2.1, Quart. J. Roy. Meteor. Soc., 143,  
574 1844–1859, <https://doi.org/10.1002/qj.3046>, 2017.
- 575 Yokoi, S., and Matsumoto, J.: Collaborative effects of cold surge and tropical depression–type  
576 disturbance on heavy rainfall in central Vietnam, Mon. Wea. Rev., 136, 3275–3287.  
577 <https://doi.org/10.1175/2008MWR2456.1>, 2008.
- 578 Yen, M.C., Chen, T.-C., Hu, H.-L., Tzeng, R.-Y., Dinh, D.T., Nguyen, T.T.T., and Wong, C.J.:  
579 Interannual variation of the fall rainfall in Central Vietnam, J. Meteor. Soc. Japan, 89A, 259-270.  
580 <https://doi.org/10.2151/jmsj.2011-A16>, 2010.
- 581 Yamada, H., Geng, B., Uyeda, H., and Tsubokoy, K.: Role of the Heated Landmass on the Evolution  
582 and Duration of a Heavy Rain Episode over a Meiyu-Baiu Frontal Zone, Journal of the  
583 Meteorological Society of Japan, Vol. 85, No. 5, 687-709, 2007.
- 584 Website:
- 585 Tuoi Tre news (2018) [https://tuoitre.vn/mien-trung-tiep-tuc-mua-lon-14-nguoi-chet-va-mat-tich-](https://tuoitre.vn/mien-trung-tiep-tuc-mua-lon-14-nguoi-chet-va-mat-tich-20181212201907413.htm)  
586 [20181212201907413.htm](https://tuoitre.vn/mien-trung-tiep-tuc-mua-lon-14-nguoi-chet-va-mat-tich-20181212201907413.htm).